

# Accepted Manuscript

Phase equilibria, microstructure, and high temperature oxidation resistance of novel refractory high-entropy alloys

B. Gorr, M. Azim, H.-J. Christ, T. Mueller, D. Schliephake, M. Heilmaier

PII: S0925-8388(14)02655-3

DOI: <http://dx.doi.org/10.1016/j.jallcom.2014.11.012>

Reference: JALCOM 32561

To appear in: *Journal of Alloys and Compounds*

Received Date: 8 October 2014

Revised Date: 30 October 2014

Accepted Date: 1 November 2014



Please cite this article as: B. Gorr, M. Azim, H.-J. Christ, T. Mueller, D. Schliephake, M. Heilmaier, Phase equilibria, microstructure, and high temperature oxidation resistance of novel refractory high-entropy alloys, *Journal of Alloys and Compounds* (2014), doi: <http://dx.doi.org/10.1016/j.jallcom.2014.11.012>

This is a PDF file of an unedited manuscript that has been accepted for publication. As a service to our customers we are providing this early version of the manuscript. The manuscript will undergo copyediting, typesetting, and review of the resulting proof before it is published in its final form. Please note that during the production process errors may be discovered which could affect the content, and all legal disclaimers that apply to the journal pertain.

# Phase equilibria, microstructure, and high temperature oxidation resistance of novel refractory high-entropy alloys

B. Gorr<sup>a\*</sup>, M. Azim<sup>a</sup>, H.-J. Christ<sup>a</sup>, T. Mueller<sup>b</sup>, D. Schliephake<sup>c</sup>, M. Heilmaier<sup>c</sup>

<sup>a</sup>*Institut für Werkstofftechnik, Universität Siegen, Paul-Bonatz-Str. 9-11, 57068 Siegen, Germany*

<sup>b</sup>*Institut für Bau- und Werkstoffchemie, Universität Siegen, Paul-Bonatz-Str. 9-11, 57068 Siegen, Germany*

<sup>c</sup>*Institut für Angewandte Materialien - Werkstoffkunde (IAM-WK), Karlsruhe Institute of Technology (KIT), Engelbert-Arnold-Str. 4, D-76131 Karlsruhe, Germany*

*\*Corresponding author: Email: [gorr@ifwt.mb.uni-siegen.de](mailto:gorr@ifwt.mb.uni-siegen.de); phone: +492717404653*

## Abstract

A new refractory high-entropy alloy system Mo-W-Al-Cr-x is proposed as a family of candidate materials for structural applications at high temperatures. Thermodynamic assessment was used to set the chemical composition of the first alloy as 20Mo-20W-20Al-20Cr-20Ti (at.%) with a calculated melting temperature of about 1700°C. A single disordered BCC phase should be stable at high temperatures between 1077°C and 1700°C. Microstructural examination and XRD results clearly show that the alloy in the as-cast condition exhibits a non-homogeneous microstructure with pronounced dendritic and interdendritic regions. Heat treatment processes, however, reveal a strong tendency of the alloy 20Mo-20W-20Al-20Cr-20Ti to homogenize. While possessing a high hardness of around 800HV, the crack-free indents allow the assumption that the alloy studied may be intrinsically ductile at room temperature. Despite the fact that the alloy possesses 40 at.% of refractory elements, high temperature oxidation tests show a surprisingly good oxidation resistance. Strategies to enhance the long-term stability of the disordered BCC phase aiming at achieving the required mechanical properties as well as optimizing the alloy's chemical composition in terms of high temperature oxidation resistance are discussed.

**Keywords:** High temperature material, High entropy alloy, Refractory element, Microstructure

**\*Corresponding author:** Email: [gorr@ifwt.mb.uni-siegen.de](mailto:gorr@ifwt.mb.uni-siegen.de)

## 1. Introduction

A new alloying concept, originally proposed by Yeh et al., induced the development of various high-entropy alloys (HEAs) [1]. For these materials, a single-phase solid solution strengthened microstructure is targeted. So far, the international activities to design, characterize, and optimize HEAs are mainly focused on the alloy system Fe-Co-Ni-Cr-x (x = Mn, Cu, Al, Ti etc.) which crystallizes in a face centered cubic (FCC) structure. For this alloy system, extensive investigations on microstructure of polycrystals as well as single crystals, phase stability, identification of hardening mechanisms, and mechanical properties at room temperature as well as at elevated temperatures have been carried out [2-7]. The second distinctive alloy family of HEAs is nearly exclusively based on refractory metals (RM), such as W, Mo, Nb, Ta, typically crystallizing in body centered cubic (BCC) structure. Due to the well-known high melting point of RM, alloys manufactured from these elements seem to be very promising for applications at very high service temperatures [8]. Outstanding values

were reported for yield strength of Nb-Mo-Ta-W and V-Nb-Mo-Ta-W alloys at temperatures of up to 1600°C [9]. To reduce the strikingly high alloy density, some heavy refractory elements were substituted by lighter elements, such as Zr and Ti [10].

In the present work, along the line of the second alloy system approach, we aim for a new high-entropy alloy system containing refractory elements. The prime incentive of this study is to develop novel high temperature materials, the alloying concept of which is generally based on alloy design principles of HEAs. The alloy system containing refractory elements should possess the following property combination: (i) a melting point exceeding those of Ni-based superalloys by at least 200K, (ii) a good long-term high temperature strength, (iii) oxidation protectiveness at temperatures of at least 1000°C, and (iv) a density  $< 10 \text{ g/cm}^3$ . In the first part of this paper, the alloy design concept will be presented. Following, the microstructure of the alloy in the as-cast condition as well as the microstructure after heat treatments will be discussed. Next, results of hardness measurements will be shown to give first insights into the ductility of the alloy at room temperature. Finally, results of oxidation experiments will be presented to allow a concise characterization of high temperature oxidation protectiveness.

## 2. Alloy design concept

The presented approach here is rather simple: four main elements will be set, building a core alloy system which may be expanded gradually by adding further alloying elements to fulfill the requirements mentioned above. Firstly, the majority of these elements should exhibit a high melting point. Secondly, most of the elements composing the HEAs to be developed should possess the same lattice structure, at least at the anticipated high temperatures, to facilitate the formation of a single-phase solid solution. With respect to these two constraints, it seems reasonable that Mo and W, both BCC, can be considered as prime candidates for the new alloy system. Due to their chemical similitude, they form a continuous solid solution [11]. Unfortunately, both, Mo and W, show a very poor high temperature oxidation resistance, so-called catastrophic oxidation, due to the formation of gaseous oxides [12]. In order to potentially enable the formation of a protective oxide scale on the metallic surface and, consequently, to ensure the alloy protectiveness, Al and Cr will be added to the core alloy system. The addition of both elements, Al and Cr, is essentially aimed at the formation of an alumina layer that maintains its highly protective properties also at temperatures above 1000°C [13]. In terms of high temperature oxidation, Cr effectively supports the formation of a continuous alumina scale in many alumina forming high temperature alloys [13]. While Cr also fulfills the requirement of having the same BCC structure as W and Mo, Al possesses the FCC lattice structure. However, it was found not only in other HEA systems such as  $\text{Al}_x\text{CoCrFeNi}$ , but also in steels that Al acts as a strong BCC stabilizer [6, 14]. Thus, it may be expected that Al addition to new refractory HEAs might not deteriorate the formation of a single phase BCC structure.

Most refractory elements exhibit a rather high density. This feature is undesirable and, consequently, confining for many practical applications. In order to reduce the density of the new alloy system further, Ti may be added. In addition, Ti possesses the BCC lattice at temperatures above 882°C. Therefore, it may be assumed that Ti additions would also in our alloy support the formation of a single BCC phase, at least at targeted temperatures beyond

about 1000°C. Thus, the first equimolar refractory high-entropy alloy proposed within the core alloy system determined previously consists of 20Mo-20W-20Al-20Cr-20Ti.

Since the alloy 20Mo-20W-20Al-20Cr-20Ti represents the first candidate from the new material family Mo-W-Al-Cr-x, it was considered indispensable to combine experimental investigations with theoretical evaluations, which use thermodynamic calculations. Table 1 shows phases which can form in the corresponding binary, ternary, quaternary, and quinary systems at 1100°C. Thermodynamic calculations were carried out using the software FactSage V6.4 in conjunction with a commercial database which includes the following elements: Mo, W, Al, Cr, Ti, O Results of these calculations clearly show that except two binary systems, Al-Ti and Mo-Al, the BCC phase is the solid-solution phase forming in all investigated combinations. In the binary Cr-Ti system, the ordered Laves phase (C15 crystal structure) can form along with the BCC phase, while two ternary systems, W-Cr-Al and Mo-Al-Ti, exhibit additional solid solution phases, designated B2B and CUB\_A15, respectively. It is obvious that all binary systems containing Al and the majority of ternary alloys with Al form intermetallic compounds, predominantly TiAl (see Table 1). Furthermore, all ternary systems containing the two elements, Ti and Al, as well as the majority of quaternary systems which include Ti and Al may form the well known TiAl intermetallic compound. It is obvious that this intermetallic compound may exhibit a very high thermodynamic stability. However, in the quinary alloy, TiAl seems to become rather unstable from a thermodynamic point of view and the BCC phase is the only phase which can form at 1100°C.

Table 1: Phases in the equimolar metallic systems

Systems	Solid-solution phases	Intermetallic compounds
Mo-W	BCC	
Mo-Cr	BCC	
Mo-Ti	BCC	
W-Cr	BCC	
W-Ti	BCC	
Cr-Ti	BCC+LAVES_C15	
Al-Ti		TiAl
Mo-Al		Mo <sub>3</sub> Al+Mo <sub>3</sub> Al <sub>8</sub>
W-Al	BCC	WA <sub>4</sub>
Cr-Al	BCC	Cr <sub>5</sub> Al <sub>8</sub>
Mo-W-Cr	BCC	
Mo-W-Ti	BCC	
Mo-Cr-Al	BCC	
Mo-Cr-Ti	BCC	
W-Cr-Ti	BCC	
W-Cr-Al	BCC+B2B	
W-Al-Ti	BCC	TiAl
Cr-Al-Ti	BCC	TiAl
Mo-Al-Ti	BCC+CUB_A15	TiAl
Mo-W-Al	BCC	Mo <sub>3</sub> Al <sub>8</sub>
Mo-W-Cr-Al	BCC	
Mo-W-Cr-Ti	BCC	
Mo-Cr-Al-Ti	BCC	

Mo-W-Cr-Ti	BCC	
Mo-W-Al-Ti	BCC	TiAl
W-Cr-Al-Ti	BCC	TiAl
Mo-W-Al-Cr-Ti	BCC	

Figure 1 shows fraction of phases which may be formed under equilibrium conditions in the alloy 20Mo-20W-20Al-20Cr-20Ti in the wide temperature range from 200°C to 2000°C. One intermetallic compound, TiAl, and four solid-solution phases, i.e. BCC, B2B, CUB, and sigma, can be formed below the melting temperature. It is worth noting that the BCC phase is the only phase that is stable between 1077°C and the melting point, while the intermetallic compound is only stable within a very narrow temperature range from 935°C to 1077°C, the CUB phase becomes thermodynamically unstable above 780°C, and both, the sigma and B2B phases seem to transform into the BCC phase above 1000°C. Most importantly, the chosen alloy has a melting point of  $T_m=1700^\circ\text{C}$  that is considerably higher (at least 250K) than those of commercial Ni-based alloys.

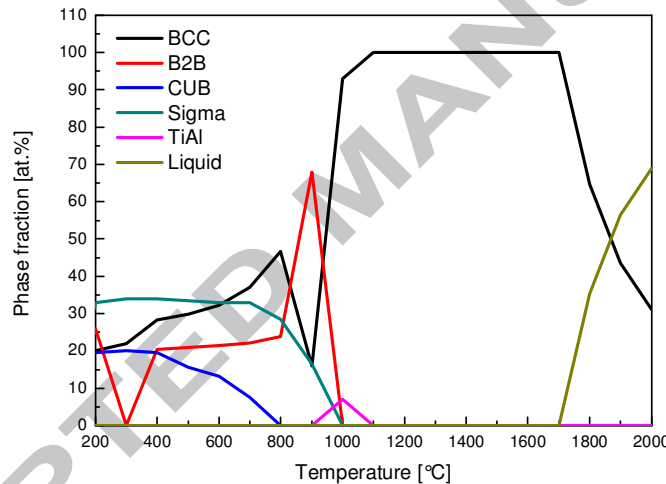


Figure 1: Equilibrium phase distribution in the alloy 20Mo-20W-20Al-20Cr-20Ti (calculated by FactSage)

Further, it is of interest to know the elemental partitioning between the phases possibly present in the alloy as shown in Fig. 1. This knowledge will be useful for further alloy development, since an undesirable phase may be eliminated by lowering the concentration of the corresponding element or even by its complete substitution by another element. Fig. 2 shows the elemental distribution in the respective phases as displayed in Fig. 1 at 700°C. Thermodynamic calculations clearly reveal that the disordered BCC phase is rich in W and Mo at this temperature, while the ordered cubic B2B phase is primarily rich in Cr. Al and Ti are the main elements present in the sigma phase, whereas the CUB phase with the ordered A15 crystal structure, generally exhibits the composition  $(\text{Mo},\text{Ti})_3\text{Al}$ , however, being enriched in Mo.

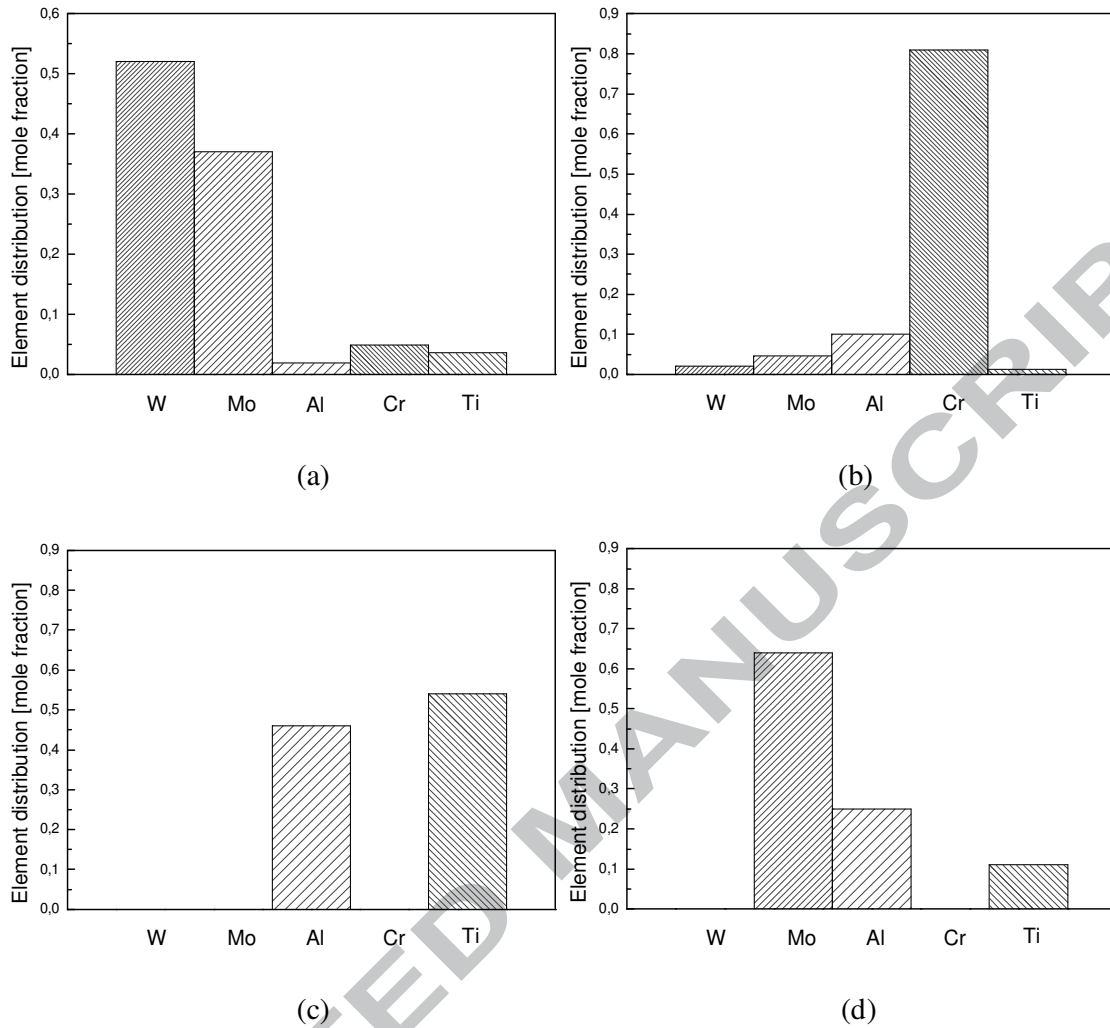


Figure 2: Element distribution in the phases of the alloy 20Mo-20W-20Al-20Cr-20Ti at 700°C; (a) BCC phase, (b) B2B phase, (c) sigma phase, and (d) CUB phase

### 3. Experimental

The alloy 20Mo-20W-20Al-20Cr-20Ti was produced from elemental bulk materials by arc-melting in ~0.6 atm of argon utilizing an arc-melter AM 0.5 by Edmund Bühler GmbH. The purities of the starting materials Mo, W, Al, Cr and Ti were 99.9%, 99.96%, 99.9%, 99% and 99.8%, respectively. Gaseous impurities such as oxygen and nitrogen were generally found to be on a very low level, with the used titanium being of significantly higher purity than commercial Ti grade 1 in particular. The prepared buttons had a mass of ~25 g and were flipped over and remelted more than five times in a water-chilled copper mold to ensure homogenization of the alloying elements. Heat treatments were carried out in protective Ar atmosphere using a tube furnace (Gero GmbH) at temperatures up to 1200°C.

The microstructure of the samples in the as-cast condition as well as after heat treatment processes was analyzed using a FIB-SEM DualBeam System of type FEI Helios Nanolab 600 equipped with BSE and EDS detector. The crystal structure was identified by using of the Panalytical X'Pert pro MPD X-ray diffractometer applying Cu K $\alpha$  radiation. Vickers

microhardness was measured on polished cross-sectional surfaces using a  $136^\circ$  Vickers diamond pyramid with a load of 100 g applied for 12s (Struers Duramin-1/-2 device). For the oxidation test, one specimen of dimension of approximately 10 mm x 10 mm x 10 mm was cut from the bar in the as-cast condition and polished up to 1000 grit. The specimen was ultrasonically cleaned in ethanol directly before testing in a Rubotherm thermogravimetric system. The morphology and composition of corrosion products was analyzed using the same experimental techniques as mentioned above.

#### 4. Results

##### 4.1 Microstructure

One of the severe limitations of the thermodynamic calculations results from the fact that they assume thermodynamic equilibrium. However, this assumption is often not fulfilled, since kinetics plays an important role in the development of the microstructure and, consequently, in determining the alloy properties. For this reason, experimental investigations on the material microstructure in different conditions, i.e. in the as-cast condition and after heat treatments, were carried out. Figure 3 shows the microstructure of the alloy 20Mo-20W-20Al-20Cr-20Ti in the as-cast condition. The alloy exhibits a dendritic microstructure which is typical of many HEAs [15]. The dendrites are slightly branched and rather rounded in shape. The EDX analysis reveals that preferentially W and partially Mo segregate to the dendrite arms, while the interdendritic regions are rich in the lighter elements Al, Cr, Ti, and, to a minor extent, in Mo (see Fig. 4). Hence, it can be assumed that the alloy in the as-cast condition either forms two phases with different crystal structures, or both dendritic and interdendritic regions possess the same crystal structure, but different chemical compositions due to segregation effects of the heavy and high melting elements, W and Mo. To clarify the last point, the cast alloy 20Mo-20W-20Al-20Cr-20Ti was solution heat treated for 20h and 40h at  $1200^\circ\text{C}$ , respectively.

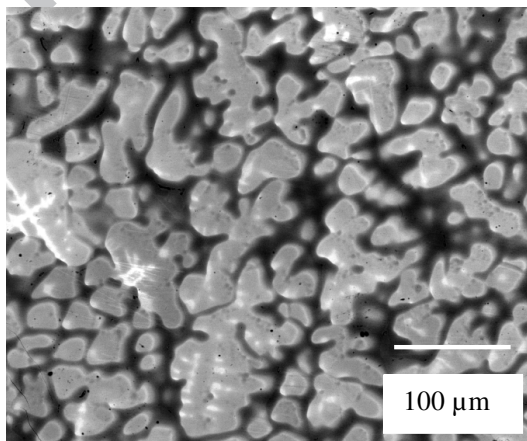


Figure 3: Microstructure of the alloy 20Mo-20W-20Al-20Cr-20Ti in the as-cast condition (SEM BSE mode)

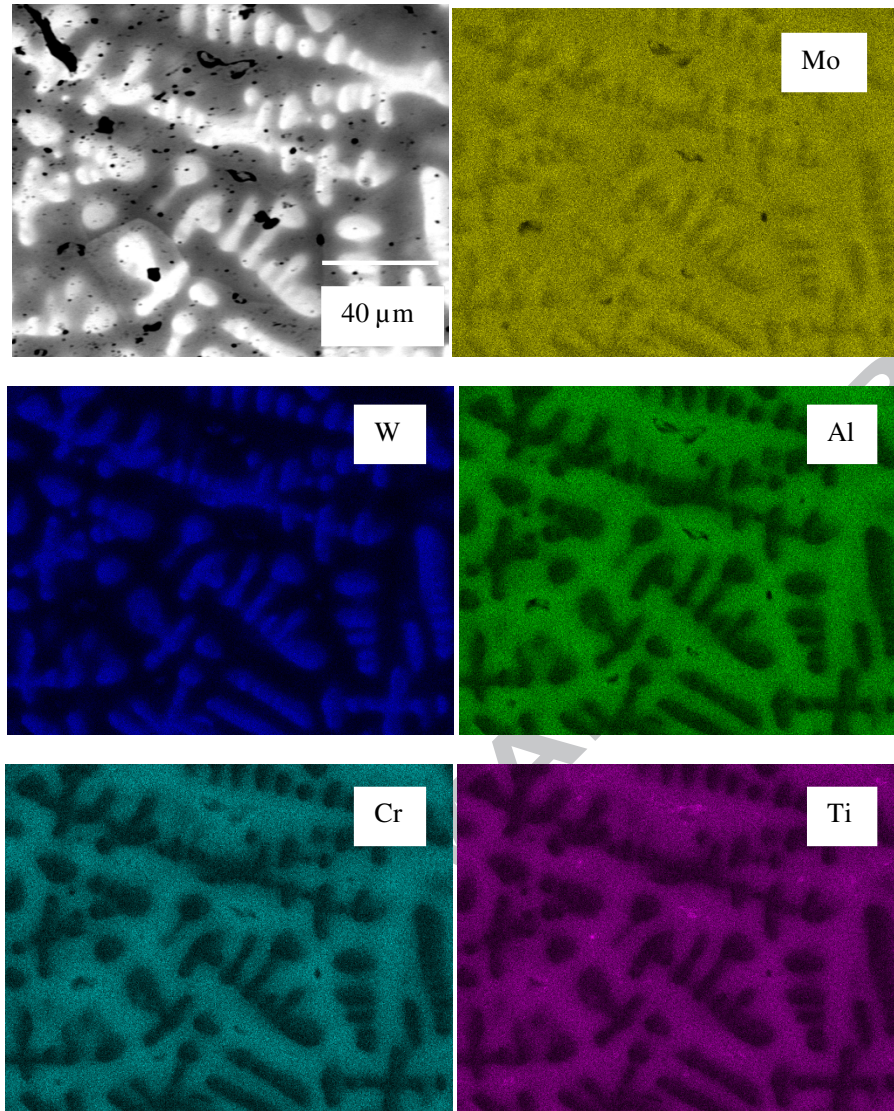


Figure 4: Element distribution in the alloy 20Mo-20W-20Al-20Cr-20Ti in the as-cast condition

Figure 5 shows the microstructure of the alloy 20Mo-20W-20Al-20Cr-20Ti after solution heat treatments at 1200°C for 20h and 40h (Fig. 5(a)) and 40h (Fig. 5(b)), respectively. It is obvious that the annealing at 1200°C leads to a pronounced homogenization of the alloy microstructure. After 20h only some small separate islands rich in W and Mo (former dendrites) are visible, with their size being substantially decreased compared to that formed in the as-cast condition (compare Fig. 3 and Fig. 5(a)). After 40h of annealing at 1200°C the alloy microstructure appears to be nearly homogeneous. Small black dots were identified as contaminations arising from the manufacturing process.

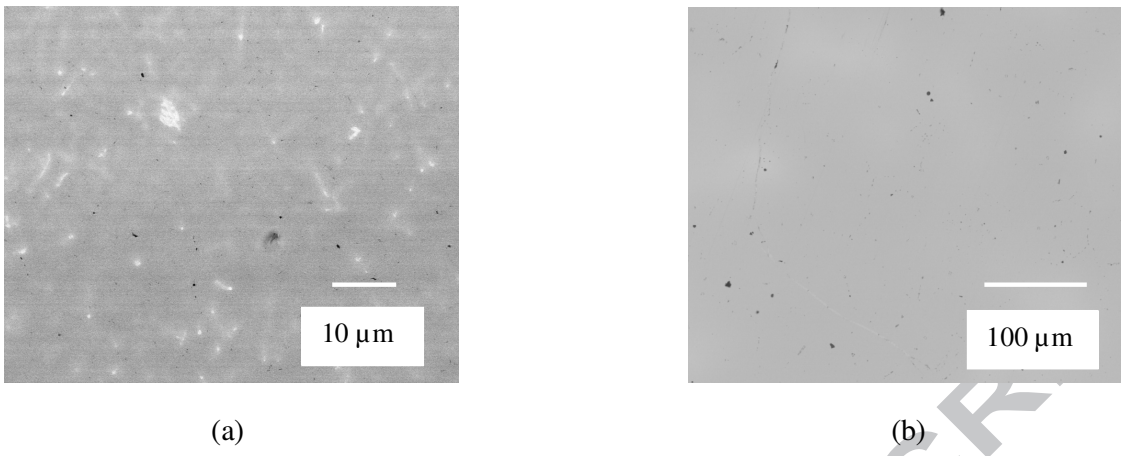


Figure 5: Effect of heat treatment processes on the microstructure of the alloy 20Mo-20W-20Al-20Cr-20Ti; (a) microstructure after 20h of heat treatment at 1200°C, (b) microstructure after 40h of heat treatment at 1200°C, both SEM BSE mode.

In order to characterize the development of the alloy microstructure further, X-ray diffraction (XRD) measurements were carried out on two samples, in the as-cast condition and after 40h of heat treatment at 1200°C, see Figure 6. Both XRD plots have been corrected for background noise and the measured intensities are plotted in a linear fashion. The analyses on both samples show five strong peaks in the  $2\theta$ -range from 15 to 120°. However, higher magnifications reveal ambiguous shoulder peaks on the left side of all diffraction peaks with high intensity (see the insertion with the higher magnification, Fig.6). To fit the peak shape, the insertion of an additional peak arranged extremely close to the main peak was necessary, indicating that the alloy in the as-cast condition as well as after the heat treatment apparently comprises two different BCC phases. One of these two BCC phases in the sample in the as-cast condition possesses a derived lattice constant of 3.1033 Å, while the second BCC phase reveals a lattice parameter of 3.116 Å. The corresponding lattice parameters determined on the sample after 40h of heat treatment at 1200°C are 3.0934 Å and 3.1015 Å for the first BCC phase and the second BCC phase, respectively. It is obvious that the marginal difference in the lattice constants between two BCC phases detected on the sample in the as-cast condition decreases further for the sample after heat treatment supporting the conclusion drawn from the thermodynamic calculations that a single BCC phase prevails after complete homogenization. The sole presence of disordered BCC phase(s) was also confirmed by additional inspection of the measured intensities in the XRD patterns by plotting on a logarithmic scale (not shown here): no additional peaks due to further phases could be detected.

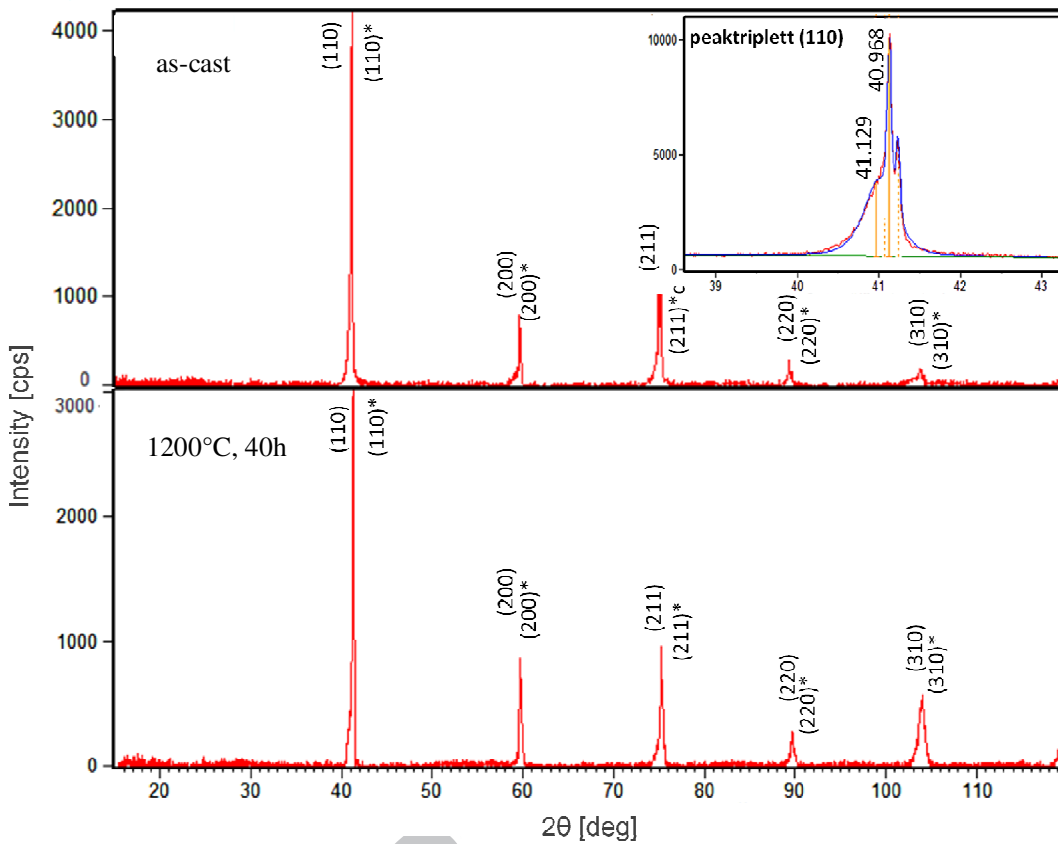


Figure 6: XRD patterns of the alloy 20Mo-20W-20Al-20Cr-20Ti: (top) in the as-cast condition and (bottom) after 40h of heat treatment at 1200°C.

#### 4.2 Hardness measurement

Hardness measurements should provide first insights into the mechanical properties of the alloy at room temperature. The hardness indentation in Fig. 7(a) exemplarily carried out on the as-cast sample clearly demonstrates the ductile nature of the alloy since cracks were neither detected in the dendrites nor in the interdendritic areas. As expected, the W- and Mo-rich dendrites exhibit much higher hardness values compared to the interdendritic areas and the spread of the hardness values is substantial. Clearly, these values can be grouped into two categories in terms of the dendritic and the interdendritic regions, respectively, as shown in Fig. 7(b). The mean hardness value of the dendrites is about 685 HV, while the corresponding value for the interdendritic regions is about 330 HV. By contrast, the hardness values measured on the sample after 40 h annealing at 1200°C lie with  $802 \pm 10$  HV<sub>0.1</sub> very close together (see Fig. 7(c)) indicating a significantly more homogeneous microstructure. These results are in good agreement with the microstructural analysis shown above.

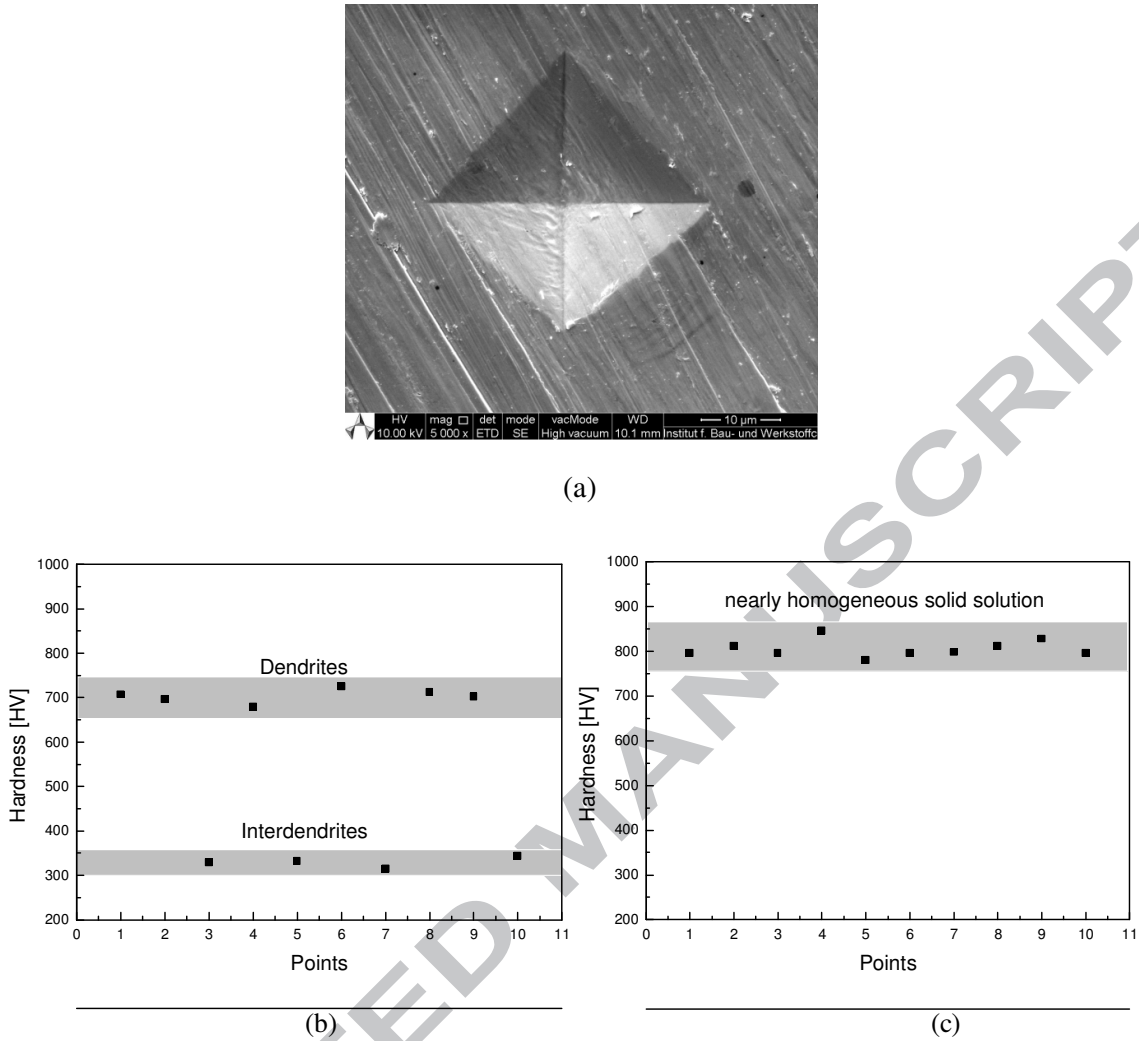


Figure 7: Hardness measurement; (a) top view of a hardness indent, (b) hardness values of the alloy 20Mo-20W-20Al-20Cr-20Ti in the as-cast condition, and (c) hardness values of the alloy 20Mo-20W-20Al-20Cr-20Ti after 40h of heat treatment at 1200°C.

#### 4.3 Oxidation behavior

As mentioned above, the oxidation behavior is a crucial feature for alloys containing refractory metals. Since the alloy 20Mo-20W-20Al-20Cr-20Ti contains 40 at.% of refractory elements (20 at.% Mo and W each), it is of interest to explore the potential of this alloy regarding the high temperature oxidation resistance. Figure 8 shows the mass change of the alloy 20Mo-20W-20Al-20Cr-20Ti in the as-cast condition during 40h of exposure to laboratory air at 1000°C. The kinetic curve obviously obeys the parabolic rate law indicating that the growth of the oxide scale proceeds through solid state diffusion. Further, considering the position of the thermogravimetric curve at positive values and its positive slope, it can be assumed that the evaporation of Mo and W oxides during the oxidation process is either negligibly small or entirely inhibited by the oxide layer formed on the metallic substrate. However, it should be pointed out that despite the parabolic trend of the kinetic curve the mass gain after 40h of exposure is significant compared to state-of-the-art Ni-based superalloys [13].

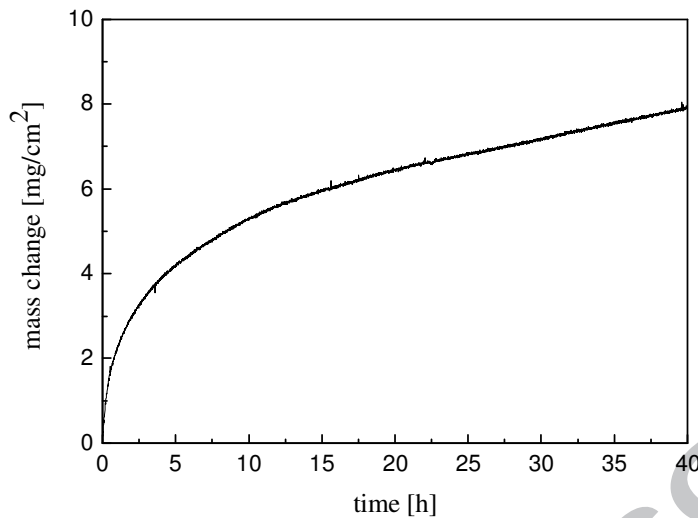
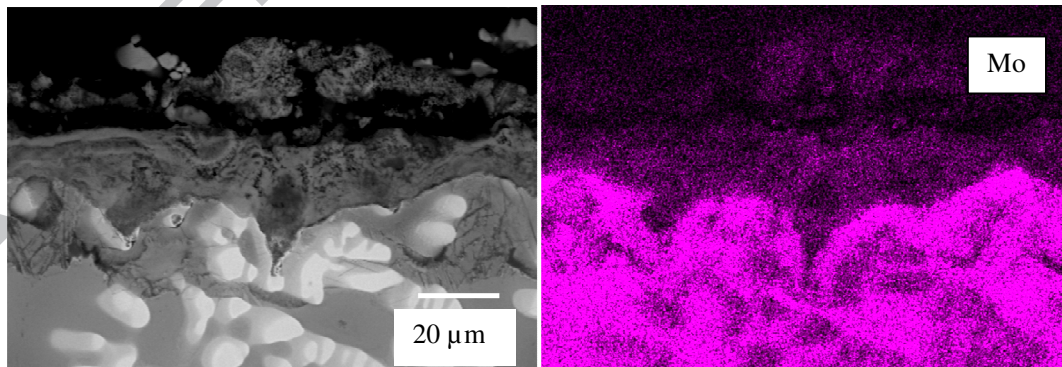


Figure 8: Mass change of the alloy 20Mo-20W-20Al-20Cr-20Ti during exposure to laboratory air at 1000°C.

Figure 9 shows micrographs of a cross-section as well as the EDX element distributions of the alloy 20Mo-20W-20Al-20Cr-20Ti after 40h exposure to air at 1000°C. The formation of a rather inhomogeneous and porous oxide scale on the surface is characteristic of the alloy. The metallic substrate is covered by a mixed oxide which primarily consists of Al, Cr, and Ti oxides. In addition, this oxide layer exhibits a slight tendency to spalling. Despite the fact that the scale formed on the surface consists of a mixed oxide, several prospective features can be found. Firstly, the thickness of the oxide scale is rather moderate (about 23µm), indicating the relatively slow diffusion rates in the oxide scale. Secondly, EDX element distribution micrographs clearly show that a semi-continuous Cr<sub>2</sub>O<sub>3</sub> scale forms on the interface oxide/substrate, underpinning the potential ability of the alloy to form a protective oxide scale. Thirdly, the EDX analysis evidently indicates that only negligibly small amounts of Mo and W were detected in the oxide scale, suggesting that the alloy does not suffer from catastrophic oxidation.



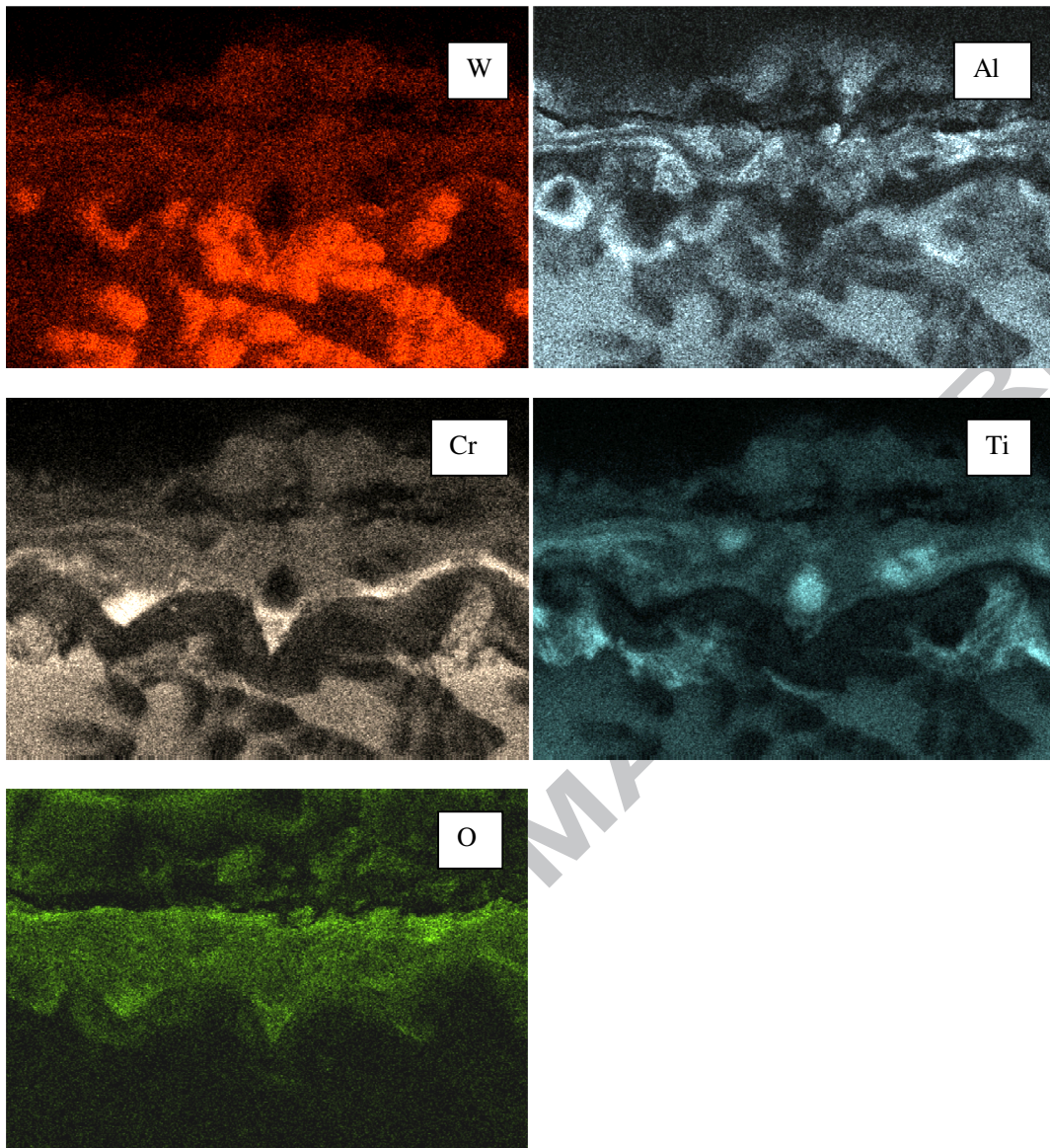


Figure 9: Cross-section and corresponding EDX element distribution micrographs of the alloy 20Mo-20W-20Al-20Cr-20Ti after exposure to laboratory air at 1000°C for 40h

## 5. Discussion

The concept of HEAs postulates the preferential formation of a disordered, ideally single-phase, solid solution microstructure in equimolar HEAs, while the formation of brittle intermetallic compounds should be inhibited in consequence of thermodynamic driving forces [1]. In reality, in addition to disordered solid solutions, HEAs quite often form other phases, such as ordered solid solutions, amorphous phases and even intermetallic compounds [4]. This may indicate that in many cases the simple HEA concept is at least debatable. The development of the alloy 20Mo-20W-20Al-20Cr-20Ti also aimed at the formation of a simple-single phase microstructure. The results of the microstructural analysis shown above reveal that our alloy obviously tends to form a disordered body centered cubic crystal structure at high temperatures upon annealing. XRD measurements clearly show that the difference in lattice constant between two crystal structures diminishes for the sample after

the heat treatment supporting the conclusion from the thermodynamic calculations that only one BCC phase should form in the alloy after appropriate heat treatment. After the applied heat treatment of 40h at 1200°C, however, the alloy still reveals inhomogeneity in the chemical composition on atomic scale due to insufficient intermixing of the atoms with substantially different radii. This can either cause locally varying lattice distortions within a single BCC phase or the presence of two BCC phases with only slightly different lattice constants. Hence, the assumed incomplete homogenization leaves potential for further optimization in order to achieve a truly single-phase and, hence, homogeneous microstructure. In this regard, further heat treatments as well as extensive microstructural investigations will be carried out in future work.

Although the alloy 20Mo-20W-20Al-20Cr-20Ti tends to possess a rather simple microstructure consisting of the two BCC phases, the thermodynamic calculations shown in Fig. 1 reveal that the formation of a small amount (about 7 at. %) of an intermetallic compound TiAl is possible within the temperature range from 935°C to 1077°C. To clarify whether TiAl forms in the alloy at 1000°C, further XRD measurements were carried out on a sample annealed for 24h at 1000°C. However, no TiAl was detected utilizing XRD which is assumed to be caused by the sluggish kinetics in this alloy at 1000°C as well as due to the relatively short time of the annealing process. Thus, the formation of the TiAl phase in the alloy seems to be inhibited.

In order to identify the critical concentration of Al that must be exceeded to suppress the intermetallic compound TiAl in the alloy 20Mo-20W-20Al-20Cr-20Ti, additional thermodynamic calculations were carried out. In these calculations, the amount of Al was varied, while the concentrations of all other elements in the alloy were kept equal and calculated as  $(100 - c^{\text{Al}})/4$ . Figure 10 proofs that the formation of the intermetallic compound TiAl can be avoided completely if the Al concentration in the alloy is set to 17 at. %.

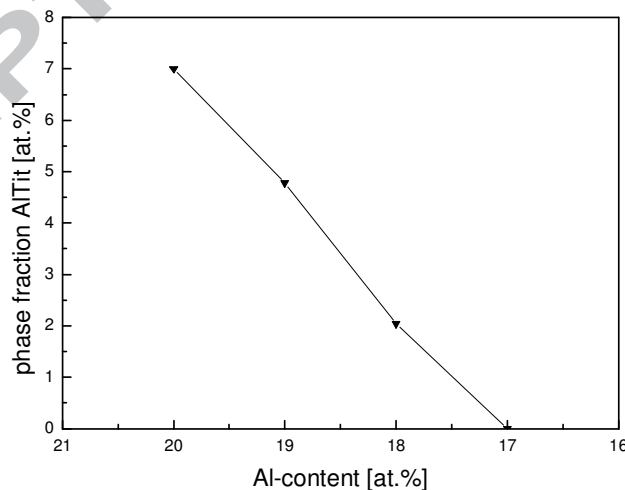


Figure 10: Change of the phase fraction of the intermetallic compound TiAl with decreasing Al content in the alloy system Mo-W-Al-Cr-Ti at 1000°C.

Likewise, Al plays an important role for the formation of the ordered CUB phase, which is found in the thermodynamic calculations to be stable in the alloy 20Mo-20W-20Al-20Cr-20Ti in the temperature range from room temperature up to 800°C. Figure 11 shows that a slight reduction of the Al content from 20 down to 17 at.% also yields a significant decrease of the phase fraction of the CUB phase, e.g. at 600°C from roughly 13 to 4 at.%. Additionally, lowering of the Al concentration in this alloy system causes a shrinkage of the field of thermodynamic stability for the CUB phase leading to a shift to lower temperatures. Since the diffusion processes are very slow at such low temperatures, the formation of the CUB phase seems to be strongly inhibited. This explains, why the phase was not observed in this study.

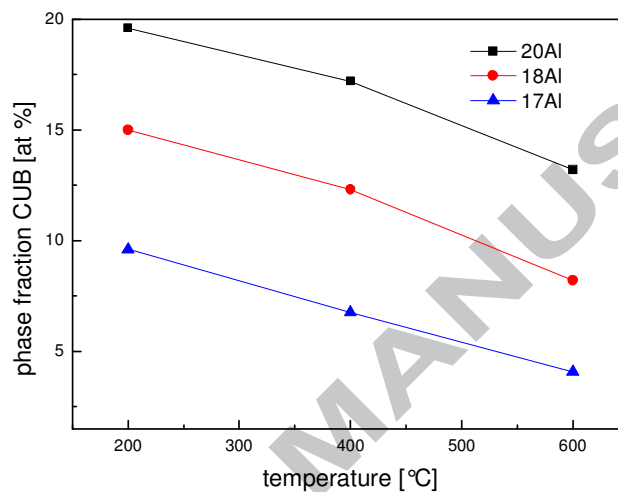


Figure 11: Effect of Al content on the phase fraction of the CUB phase in the alloy system Mo-W-Al-Cr-Ti at different temperatures

On the one hand, the results of thermodynamic calculations regarding the Al effect on the phase stability in the alloy system Mo-W-Al-Cr-Ti indicate that lowering the Al concentration may be beneficial in terms of the alloy microstructure since the amount of the TiAl and CUB phases can be reduced significantly or their formation can even be suppressed. On the other hand, besides the suppression of some ordered phases, the formation of the disordered BCC solid solution was of paramount importance. Figure 12 shows the effect of the Al content on the Gibbs free energy of the BCC phase within the temperature range from 200 to 1700°C. Clearly, the calculated increase of the Gibbs free energy with decreasing Al concentration is marginal. Thus, it can be assumed that lowering of the Al content in the alloy system Mo-W-Al-Cr-Ti, at least from 20 to 17 at.%, will cause no significant change of the thermodynamic stability of the disordered BCC phase.

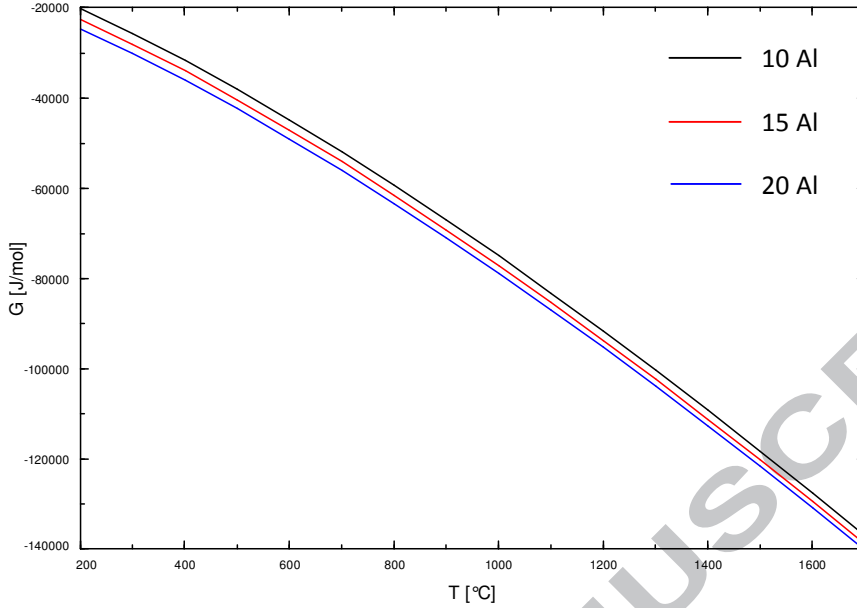


Figure 12: Effect of Al content on the Gibbs energy of the BCC phase in the alloy system Mo-W-Al-Cr-Ti at different temperatures

High temperature oxidation experiments displayed that though the oxidation kinetics follows the parabolic rate law, the oxidation rate is rather high. In fact, the high temperature oxidation resistance of the alloy 20Mo-20W-20Al-20Cr-20Ti may be improved by the formation of a dense and continuous oxide layer, either  $\text{Al}_2\text{O}_3$  or  $\text{Cr}_2\text{O}_3$ . The cross-sectional analysis of an oxidized sample (Fig. 9) clearly reveals that no protective oxide scale, neither  $\text{Al}_2\text{O}_3$  nor  $\text{Cr}_2\text{O}_3$ , is formed on the metallic surface. While a discontinuous layer of  $\text{Cr}_2\text{O}_3$  is clearly visible at the interface oxide/substrate,  $\text{Al}_2\text{O}_3$  was only found as a constituent of the thick oxide scale that represents a mixture of diverse oxides, such as  $\text{TiO}_2$ ,  $\text{Al}_2\text{O}_3$ ,  $\text{Cr}_2\text{O}_3$ ,  $\text{WO}_3$  etc. Numerous studies on high temperature oxidation behavior of different alloys concluded that the formation of a highly protective oxide layer consisting of a single oxide is substantially impeded if oxides form, which exhibit similar thermodynamic stabilities. It is, for example, surprising that TiAl alloys containing high Al concentrations from 35 at.% to 50 at. % do not form a protective  $\text{Al}_2\text{O}_3$  scale. Instead, a thick and porous oxide layer consisting of a mixture of  $\text{Al}_2\text{O}_3$  and  $\text{TiO}_2$  forms on the metallic surface leading to high oxidation rates [16]. Here, both oxides,  $\text{Al}_2\text{O}_3$  and  $\text{TiO}_2$ , show very similar thermodynamic stabilities and, thus, the same behavior prevails in the alloy 20Mo-20W-20Al-20Cr-20Ti.

Becker et al. investigated the effect of different additional elements on the oxidation protectiveness of TiAl alloys. It was found that only Nb containing alloys formed a long-lasting, protective  $\text{Al}_2\text{O}_3$  layer [16]. Stroosnijder et al. reported the strong beneficial effect of Nb ion implantation on the high temperature oxidation resistance of the  $\gamma$ -TiAl-based alloy Ti-48Al-2Cr [17]. This process facilitates the formation of a  $\text{Al}_2\text{O}_3$  scale notably enhancing the oxidation protectiveness of the alloy. One can speculate whether Nb has the same positive effect on the oxidation behavior of the alloy 20Mo-20W-20Al-20Cr-20Ti. In addition, Nb exhibits a BCC crystal structure as most of the elements in the alloy 20Mo-20W-20Al-20Cr-

20Ti. Thus, it can be supposed that no additional complex phases form in the alloy. Further, thermodynamic assessments as well as ensuing experiments will be needed to verify these hypotheses.

## 6. Conclusions

In this paper, a new refractory high-entropy alloy system Mo-W-Al-Cr-x was proposed as a perspective candidate for applications at high temperatures. Neither thermodynamic nor experimental data have been published yet on this system. The alloy 20Mo-20W-20Al-20Cr-20Ti from this system was investigated with respect to phase stability, alloy microstructure, mechanical properties at room temperature, and high temperature oxidation behavior. The following characteristics of this alloy can be summarized:

1. Thermodynamic calculations were used as a powerful means to define and confirm the suitable chemical composition of the alloy 20Mo-20W-20Al-20Cr-20Ti. The calculated melting temperature of the alloy is about 1700°C. According to the results of the thermodynamic calculations, the BCC phase is the only phase which is stable at temperatures above 1100°C. Three solid solutions and the intermetallic compound TiAl possibly form at lower temperatures. A reduction of the Al content in the alloy down to 17 at. % would, however, entirely prevent the formation of the intermetallic compound TiAl. Additionally, the reduction of the Al concentration may induce a significant decrease of the phase fraction of the ordered CUB phase. Concurrently, the thermodynamic stability of the solid-solution BCC phase seems to remain nearly unaffected.
2. The alloy exhibits a dendritic microstructure in the as-cast condition which is typical of many HEAs. Microstructural analysis reveals that preferentially W and partially Mo segregate to dendrites, while the interdendritic regions are rich in Al, Cr, Ti, and, to some extent, in Mo. The corresponding heat treatments lead to a homogenization of the alloy. XRD measurements show that either two BCC phases with slightly different lattice constants or even one BCC phase with a fluctuating lattice distortion form in the alloy in the as-cast conditions as well as after homogenization. This can probably be attributed to the incomplete homogenization of the alloy after annealing. Further investigations are needed to solve this issue.
3. Hardness measurements of the sample in the as-cast condition show a bifurcation of the hardness values depending on whether dendritic or interdendritic regions were probed, while the hardness values of the sample after annealing are constant with  $802 \pm 10$  HV. In addition, the hardness indentations reveal no cracks in both, the dendritic and interdendritic areas, indicating the potentially ductile behavior of the alloy at room temperature.
4. Although many materials containing refractory metals suffer from severe oxidation, the alloy already reveals a surprisingly good high temperature oxidation resistance. The mass change of the alloy during 40h of exposure to air at 1000°C follows the parabolic rate law indicating that the growth of the oxide scale proceeds through solid state diffusion. The evaporation of oxides of refractory elements Mo and W seems to be either negligibly small or entirely inhibited by the oxide layer formed on the alloy. Nevertheless, the oxidation rate is still relatively high. A substitution of Ti by Nb in

the alloy may facilitate the formation of a protective  $\text{Al}_2\text{O}_3$  on the metallic substrate, improving the oxidation resistance notably.

## 7. References

- [1] J.W. Yeh, S.K. Chen , S.J. Lin, J.Y. Gan, T.S. Chin, T.T. Shun, C.H. Tsau, S.Y. Chang: Nanostructured high-entropy alloys with multiple principal elements, Novel alloy design, concepts and outcomes, *Adv. Eng. Mater.* 6 (2004) 299-303.
- [2] M.R. Chen, S.J. Lin, J.W. Yeh, S.K. Chen, Y.S. Huang, C.P. Tu, Microstructure and properties of  $\text{Al}_{0.5}\text{CoCrCuFeNiTi}_x$  ( $x=0-2.0$ ) high-entropy alloys, *Mat. Trans.* 47 (2006) 1395-1401.
- [3] S.G. Ma, S.F. Zhang, M.C. Gao, P.K. Liaw, Y. Zhang, A successful synthesis of the  $\text{CoCrFeNiAl0.3}$  single-crystal, high-entropy alloy by Bridgman Solidification, *JOM* 65 (2013) 1751-1757.
- [4] S. Guo, C.T. Liu, Phase stability in high entropy alloys: Formation of solid-solution phase or amorphous phase, *Prog. Nat. Sci.* 21 (2011) 433-446.
- [5] Y.J. Zhou, Y. Zhang, Y.L. Wang, G.L. Chen, Microstructure and compressive properties of multicomponent  $\text{Al}_x(\text{TiVCrMnFeCoNiCu})_{100-x}$  high-entropy alloys, *Mater. Sci. Eng. A* 454-455 (2007) 260-265.
- [6] C. Zhang, F. Zhang, S. Chen, W. Cao, Computational thermodynamics aided high-entropy alloy design, *JOM* 64 (2012) 839-845.
- [7] C.J. Tong, M.R. Chen, S.K. Chen, J.W. Yeh, T.T. Shun, S.J. Lin, S.Y. Chang, Mechanical performance of the  $\text{Al}_x\text{CoCrCuFeNi}$  high-entropy system with multicomponent elements, *Metall. Mat. Trans. A* 36A (2005) 1263-1271.
- [8] O.N. Senkov, G.B. Wilks, D.B. Miracle, C.P. Chuang, P.K. Liaw, Refractory high-entropy alloys, *Intermetallics* 18 (2010) 1758-1765.
- [9] O.N. Senkov, G.B. Wilks, J.M. Scott, D.B. Miracle, Mechanical properties of  $\text{Nb}_{25}\text{Mo}_{25}\text{Ta}_{25}\text{W}_{25}$  and  $\text{V}_{20}\text{Nb}_{20}\text{Mo}_{20}\text{Ta}_{20}\text{W}_{20}$  refractory high entropy alloys, *Intermetallics* 19 (2011) 698-706.
- [10] O.N. Senkov, J.M. Scott, S.V. Senkova, D.B. Miracle, C.F. Woodward, Microstructure and room temperature properties of a high-entropy  $\text{TaNbHf ZrTi}$  alloy, *J. Alloys Compd.* 509 (2011) 6043-6048.
- [11] Landolt-Börnstein: Binary systems. Part 4: Binary systems from Mn-Mo to Y-Zr. Phase diagrams, phase transition data, integral and partial quantities of alloys, Springer Berlin Heidelberg, 2006.
- [12] P. Kofstad, High temperature oxidation of metals, John Wiley and Sons, Inc., New York, USA, 1966.
- [13] D. J. Young, High temperature oxidation and corrosion of metals, Elsevier, New York, 2010.

- [14] Z. Tang, M.C. Gao, H. Diao, T. Yang, J. Liu, T. Zuo, Y. Zhang, Z. Lu, Y. Cheng,, Y. Zhang, K. A. Dahmen, P.K. Liaw, T. Egami, Aluminium alloying effects on lattice types, microstructures, and mechanical behavior of high-entropy alloys systems, *JOM* 65 (2013) 1848-1858.
- [15] B. Cantor, I.T.H. Chang, P. Knight, A.J.B. Vincent, Microstructural development in equiatomic multicomponent alloys, *Mater. Sci. Eng. A* 375-377 (2004) 213-218.
- [16] S. Becker, A. Rahmel, M. Schorr, M. Schütze, Mechanism of isothermal oxidation of the intermetallic TiAl and of TiAl alloys, *Oxid. Met.* 38 (1992) 425-464.
- [17] M.F. Stroosnijder, N. Zheng, W.J. Quadakkers, R. Hofman, A. Gil, F. Lanza, The effect of niobium ion implantation on the oxidation behavior of a  $\gamma$ -TiAl-based intermetallics, *Oxid. Met.* 46 (1996) 19-35.

**Highlights**

- A new candidate for applications at high temperature is proposed.
- The calculated melting point of the alloy is 1700°C
- The alloy possesses a simple microstructure.
- The alloy exhibits perspectives in terms of mechanical properties and oxidation resistance.